Available online at www.sciencedirect.com
SCIENCE DIRECT®
Journal of Nuclear Materials 336 (2005) 210–216
journal of nuclear materials
www.elsevier.com/locate/jnucmat

Role of nickel in a semi-mechanistic analytical model for radiation embrittlement of model alloys

L. Debarberis [a,*], B. Acosta [a], F. Sevini [a], A. Kryukov [b], F. Gillemot [c], M. Valo [d], A. Nikolaev [e], M. Brumovsky [f]

[a] *Joint Research Centre of the European Commission, Institute for Energy, P.O. Box 2, 1755 ZG Petten, The Netherlands*
[b] *Russian Research Centre Kurchatov Institute, Kurchatov Square 1, 123182 Moscow, Russia*
[c] *AEKI Atomic Research Institute, Konkoly Thege M. út 29-33, 1121 Budapest, Hungary*
[d] *VTT, Otakaari 3A, 02044 Espoo, Finland*
[e] *CRISM 'Prometey', 49 Shpalernaya Street, 191015 St. Petersburg, Russia*
[f] *NRI, Nuclear Research Institute, Husinec - Rez 130, 25068 Rez, Czech Republic*

Received 6 April 2004; accepted 9 October 2004

Abstract

A model based on key embrittlement mechanisms is proposed for the analysis. The advantages of such semi-mechanistic model, when compared to non-mechanistic models, is that it allows improved fitting of data and permits the visualization of the relative contribution to embrittlement of the various damage components. Data from a set of model alloys with parametric variation of the Cu, P and Ni contents, irradiated in the High Flux Reactor Petten (The Netherlands) and Kola Nuclear Power Plant (Russia), have been thoroughly analysed. The low Ni model alloys results are studied in detail showing the semi-mechanistic model capabilities and their potential for application to commercial steels and welds; in particular for those used in Russian pressure water reactor (VVER). The additional effect of Ni and its influence in the model are also presented in this article.

1. Key embrittlement mechanisms

General agreement exists on three basic mechanisms contributing to primary radiation embrittlement (occurring before vessel annealing) for of steels and welds: matrix damage, irradiation induced precipitation and elements segregation. In spite of this fact the models for analysis of radiation embrittlement are mainly based on statistical correlation of large sets of data. The key embrittlement mechanisms taking place during irradiation of reactor pressure vessel (RPV) steels and welds [1] that are considered in this paper are summarized in Table 1.

As neutrons interact with the crystalline structure of the steel, the ferrite matrix is directly damaged. In a given material, temperature and stress state matrix damage can be assumed to be simply dependent on fluence. At higher irradiation temperatures, the rate of damage is considered to be decreasing due to increased mobility of atoms. During matrix damage formation, copper together with other elements is known to lead precipitation of nano-precipitates also inducing matrix hardening and embrittlement. This precipitation effect is expected to

* Corresponding author. Tel.: +31 224 565130; fax: +31 224 565636.
E-mail address: luigi.debarberis@cec.eu.int (L. Debarberis).

0022-3115/$ - see front matter © 2004 Elsevier B.V. All rights reserved.
doi:10.1016/j.jnucmat.2004.10.002

Table 1
Embrittlement mechanisms considered

Embrittlement mechanism	Remarks
Matrix damage	Due to formation of vacancies, interstitials, dislocation loops, etc.
Precipitation hardening the matrix	Cu is the leading element
Segregation	P is a recognized segregating element

saturate due to the progressive reduction of available precipitable elements in solid solution. Such effect is related in particular with the copper concentration. In addition, other elements, like P, can segregate inside the grains (i.e. at dislocation planes), interacting with matrix defects (i.e. vacancies, interstitials, dislocation loops) or may be attracted to the Cu-type precipitates. Phosphorus also migrates to grain boundary through diffusion processes.

In the following, the analytical embrittlement model based on the above-mentioned key mechanisms is reviewed.

2. Semi-mechanistic model

The contribution of the various mechanisms to embrittlement expressed in terms of ductile-to-brittle transition temperature shift ($DBTT_{shift}$) is considered to be additive. Matrix damage contribution, assumed to have a square root dependence on fluence, is then described as follows:

$$DBTT_{shift\,matrix} = a \cdot \Phi^{n}, \tag{1}$$

where $DBTT_{shift\,matrix}$ is the transition-temperature shift component due to matrix damage, Φ is the neutron fluence ($10^{18}\,n\,cm^{-2}$), a is a model fitting parameter and n is the exponent (normally 1/2). The parameter$a$ is constant for a given material and decreases with increasing irradiation temperature.

In addition to matrix damage during the primary embrittlement, copper is known to lead the precipitation mechanism of nano-precipitates also inducing matrix hardening and embrittlement. Such precipitation mechanism continues until saturation depending on the available copper amount [2]. The contribution to the total transition-temperature shift can be described as

$$DBTT_{shift\,Cu\,precipitation} = b \cdot [1 - e^{-\Phi/\Phi_{sat}}], \tag{2}$$

where $DBTT_{shift\,Cu\,precipitation}$ is the transition temperature shift component due to Cu precipitation, b is a model fitting parameter representing the maximum saturation value of the shift due to precipitation, Φ is the neutron fluence ($10^{18}\,n\,cm^{-2}$) and Φ_{sat} is a model fitting parameter describing the start of saturation in $DBTT_{shift}$ (in practice, it is the fluence at which 66% of the asymptotic value of $DBTT_{shift}$ is reached).

Other segregates, mainly phosphorus, can be formed afterwards both interacting with already formed matrix defects and attracted into the Cu precipitates [3]. Diffusion of segregates plays also a role. A simple model to describe generally this additional contribution to $DBTT_{shift}$ is proposed based on a 'hyperbolic tangent' shape function. In this way the small increase rate of $DBTT_{shift}$ with the fluence at beginning of the process and the subsequent gradual rise approaching saturation are described by

$$DBTT_{shift\,P\,segregation} = c \cdot \left[0.5 + 0.5 \cdot \tanh\left(\frac{\Phi - \Phi_{start}}{d}\right)\right], \tag{3}$$

where $DBTT_{shift\,P\,segregation}$ is the transition-temperature shift component due to P segregation, c is a model fitting parameter representing the saturation value of the shift due to segregation, Φ is the neutron fluence ($10^{18}\,n\,cm^{-2}$), Φ_{start} is a model parameter, representing the fluence at which segregation starts, and d is a model parameter representing the velocity of rising of $DBTT_{shift}$ until the saturation value is reached.

Based on the above-mentioned partial effects, the total effect in term of transition temperature shift is

$$DBTT_{shift} = a \cdot \Phi^{n} + b \cdot [1 - e^{-\Phi/\Phi_{sat}}] + c \cdot \left[0.5 + 0.5 \cdot \tanh\left(\frac{\Phi - \Phi_{start}}{d}\right)\right]. \tag{4}$$

An example of primary radiation embrittlement calculated with the proposed model is given in Fig. 1.

A maximum of six parameters are required in total for the proposed model: a, b, Φ_{sat}, c, Φ_{start}, d. Some parameters are of secondary importance (Φ_{sat}, Φ_{start} and d) and can be derived or fixed depending on the general behaviour of the data set to be analysed. The most important parameters are a, b, and c. Parameter b depends mainly on the Cu content and c on the P content. The relative contribution of the various damage components can be also visualized in Fig. 1. The proposed model is suited in particular for analysing data sets not really showing a simple power-type function, as it is the case in some real surveillance data sets.

3. Model applied to data from model alloys

The proposed model is tested on available data of model alloys. Model alloys have concentration variations of Cu, P and Ni and are particularly of interest for embrittlement studies. A set of model alloys have

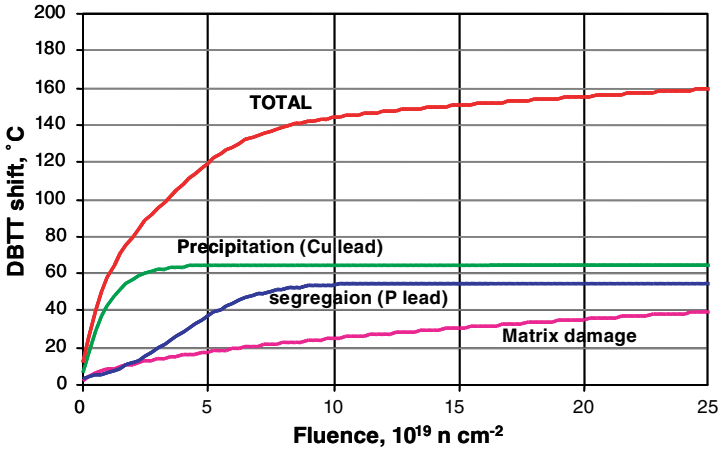

Fig. 1. Schematic of primary radiation embrittlement calculated with the proposed model.

been irradiated in the High Flux Reactor (HFR) Petten (The Netherlands) [4] and tested afterwards. The material composition, the full description of the irradiation campaign and the obtained results are given in [5]. Such model alloys already demonstrated to be a good qualitative representation of the materials used in Russian reactors VVER-440 [6] even if they may differ quantitatively in terms of higher response to radiation at relatively lower fluence. A second set of model alloys has been irradiated in Kola Nuclear Power Plant (Russia) at higher fluences, the data became recently available.

Both irradiations were carried out at 270 °C. The obtained accumulated fluences in the HFR and Kola NPP were $\approx 6.9 \times 10^{18}\,n\,cm^{-2}$ and $\approx 65 \times 10^{18}\,n\,cm^{-2}$, respectively. The DBTT shifts obtained at the HFR ranged from few degrees for very clean alloys up to more than 250 °C for alloys with very high combined contents of Cu and P. For the Ni-free alloys (≈0.004 wt%), the shifts obtained in Kola NPP were just slightly larger, in spite of the much higher fluence, than those obtained at HFR. For the alloys with higher Ni content (ranging from 1.2 to 2 wt%) much larger shifts were obtained in Kola NPP.

The semi-mechanistic model proposed in Eq. (4) was tested at first instance and parameters were fitted using the data from the model alloys with low Ni content, 22 data sets in total. Then the data from high Ni model alloys, 14 sets, have been added.

Taking the Ni-free sets, first the data on alloys with low P contents (<0.012 wt%) have been analysed in order to discriminate the effect of Cu and related parameters; see for example Fig. 2. Subsequently, the additional effect of phosphorus has been analysed considering the alloys containing P at different Cu levels. The segregation parameters have been obtained by fitting the data, see Fig. 3.

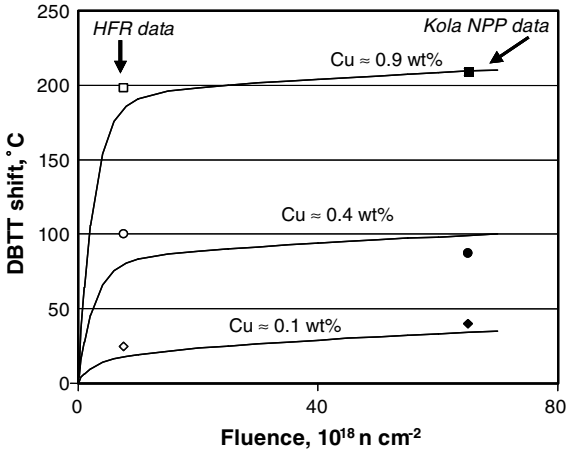

Fig. 2. Model fitting on P free alloys.

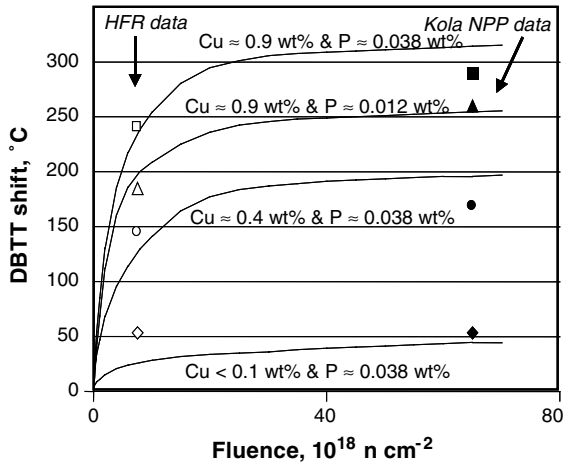

Fig. 3. Model fitting on P rich alloys; additional effect of P.

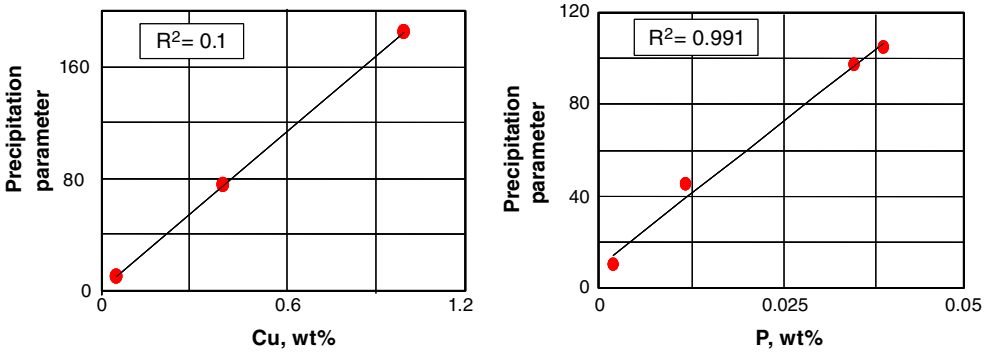

Fig. 4. Model parameters; linearly related to Cu and P contents.

The proposed model can be optimised to fit the complete data results of Ni-free alloys at both fluences. As expected the model parameters for precipitation and segregation are respectively directly related to the Cu and P contents. The observed relationships are linear ($b = 180 \cdot \mathrm{Cu}$; $c = 2857 \cdot \mathrm{P}$, Cu and P in wt%) as it is shown in Fig. 4, which reinforces the confidence in the validity of the proposed model.

The overall capability of the model to predict the behaviour of the eleven model alloys with low nickel at the two fluences is summarised in Fig. 5. The standard error of the estimated $\mathrm{DBTT}_{\mathrm{shift}}$values is 22.7 °C. The standard deviation of the residual values, see Fig. 6, amounts to 21.6 °C for this model.

The fitting could be further improved by enhancing regression with weighting factors for the few data points with larger uncertainties than others, but for the scope of this work the results are more than satisfactory and real improvement will be obtained by producing new sets of data at lower fluences, below the actual value of the HFR fluence.

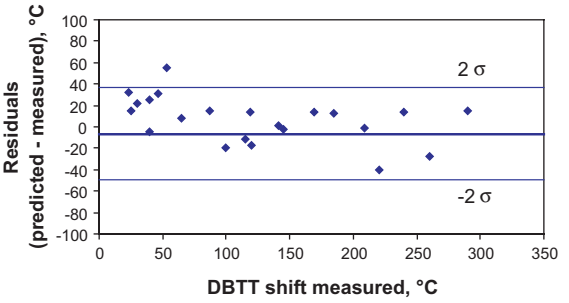

Fig. 6. Analysis of residuals for Ni-free alloys.

4. Ni effect and related modelling

The high nickel data show in comparison to the low-Ni case larger DBTT shifts and higher rates of increase; as shown for example in Fig. 7 in which model alloys

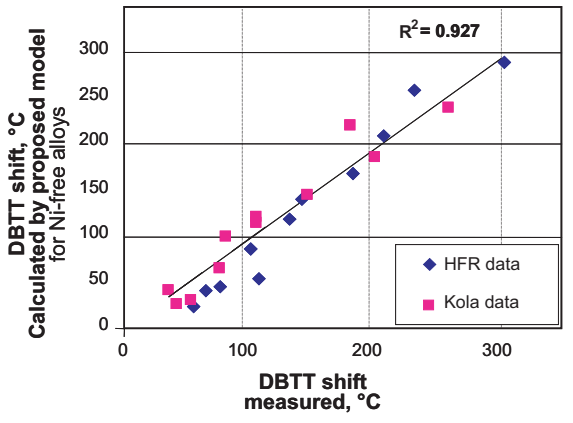

Fig. 5. Model prediction versus measured DBTT shifts (all alloys, two fluences).

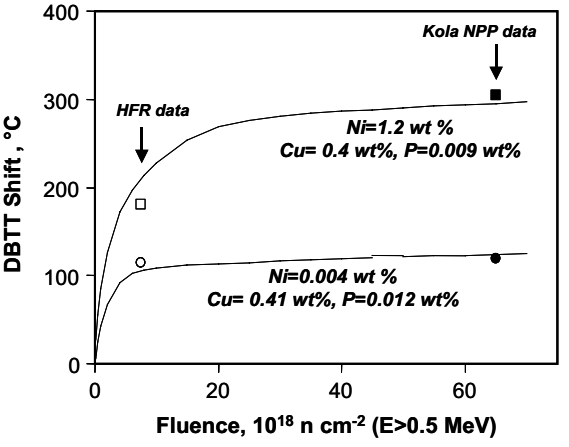

Fig. 7. Comparison of the fluence dependence of DBTT in alloys with different Ni contents.

with the same level of Cu and P but different Ni contents are compared.

In order to reproduce the observed data with the semi-mechanistic model presented in Eq. (4), we need to make the hypothesis that Ni influences one or more coefficients of the equations. Nickel could increase the matrix damage coefficient for example; in fact the structure of the material is changing by adding Ni so that the material may have different response to the matrix damage rate. Nickel has an influence on the precipitation and segregation coefficients enhancing the size of the DBTT shift attributed to such effects. Finally Ni could have an influence on the fluence at which saturation of the precipitation process begins.

In order to explain the available data sets at low and high Ni, we have to assume from the first evaluation, that Ni increases the matrix damage coefficient and strongly enhances the precipitation parameter (synergism with copper). Due to the fact that only two fluence values are available, the dependences of the saturation parameters (e.g. Φ_{sat}) on Ni are not clearly defined, and for this analysis such parameters are in fact considered fixed constants. Based on this, a simple linear dependence of the matrix damage parameter (a in Eq. (4)) on Ni content is chosen, whereas a power law dependence of the precipitation parameter (b in Eq. (4)) on Ni content is assumed:

$$a = 3 \cdot (\mathrm{Ni} + 7.5) \text{ for } \mathrm{Ni} > 0.1\,\mathrm{wt\%}, \quad (5)$$

$$b = 180 \cdot \mathrm{Cu} \cdot \mathrm{Ni}^{0.35} \text{ for } \mathrm{Ni} > 1\,\mathrm{wt\%}, \quad (6)$$

where Cu and Ni are the concentrations in wt%.

With these assumptions it is possible to model the high-nickel data (14 sets) using Eq. (4). As shown in Fig. 8, a rather good fit also to the high-Ni model alloys data is obtained, with an R^2 for the DBTT_{shift} model of 0.9. Taking into account the Ni contribution the standard error of estimate is 28 °C for the model proposed in Eq. (4). The standard deviation of the residual values is 27.9 °C in this case. The analysis of residuals when applying Eq. (4) to all model alloy data (36 data) is shown in Fig. 9, using a scatter band of $\pm 2\sigma$.

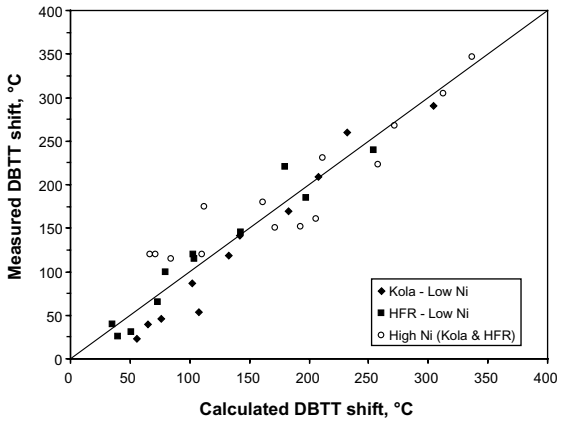

Fig. 8. Model prediction versus measured DBTT shifts; including high Ni data.

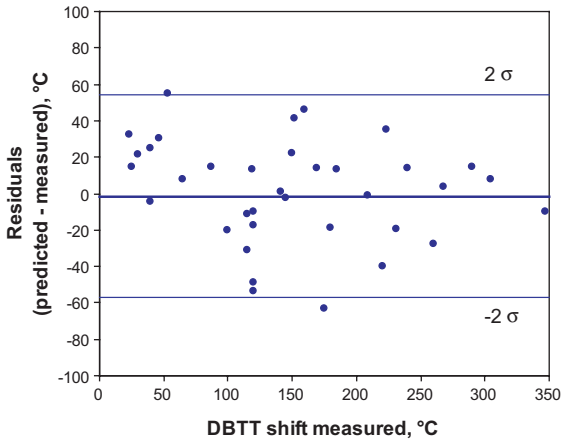

Fig. 9. Analysis of residuals for the model including Ni contribution.

Segregation should also be influenced by nickel, however, in order to determine the Ni effect on the segregation parameter c in Eq. (4), further studies are required.

5. Discussion

Based on these key mechanisms, an embrittlement model is suggested and described in Eq. (4). This proposed semi-mechanistic model allows improved fitting of data, permits the visualization of the relative contribution of the various damage components enabling better verification of the hypothesis on the relative importance of the mechanism in the different embrittlement phases, and it is suited in particular for analysing data sets which do not really show a power-type function.

The results demonstrate the following:

1. The presence of nickel always shows a clear negative influence on increasing DBTT shifts, supporting embrittlement models where Ni enhances the damage due to P and Cu (synergism).
2. Higher nickel content induces faster increase with fluence of the ductile-to-brittle transition temperature shift.

The necessity and the advantage of including nickel into the semi-mechanistic modelling of the DBTT_{shift}, as a factor enhancing both the matrix damage term and the effects of precipitations, are clearly shown in

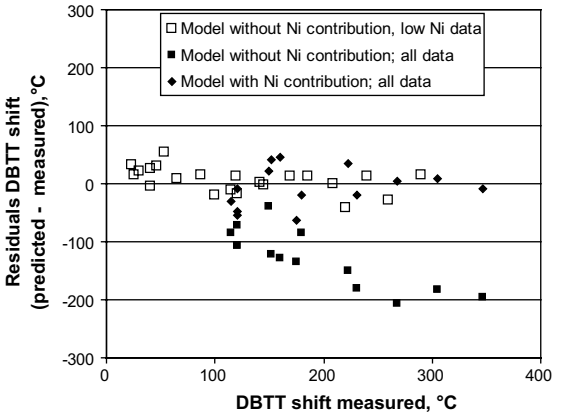

Fig. 10. Comparison of residuals by fitting models with the Ni contribution and without Ni contribution.

Fig. 10. In fact, if Ni would not be included for the higher nickel alloys (filled square symbols in Fig. 10) large underestimation of the DBTT shift (up to 200 °C divergence, which is almost 10 times the standard error) could be made in calculating the larger DBTT shifts. Hence, not taking into account the nickel contribution in the model will lead to a non-conservative prediction of the DBTT shift.

Furthermore, the hypothesis on the peculiar behaviour of re-embrittlement of high phosphorus materials, like some VVER-440 high P welds, has been better analysed in Ref. [7] using our semi-mechanistic model. What in fact is observed in the mentioned welds [8,9] is the embrittlement kinetics after vessel annealing which is different from the primary embrittlement (before annealing) kinetics: the embrittlement seems to start with a certain delay and increases rapidly afterwards; mainly the transition-temperature shift is strongly correlated with the P content and not with the Cu content. Such behaviour is supported by microstructural investigations indicating that phosphorus massively re-solutes during annealing and is almost fully available for the re-embrittlement (some will not re-solute and a fraction might reach grain boundaries). Copper, which does not re-solute in the same way, would therefore contribute marginally to re-embrittlement [10]. Using the semi-mechanistic model it is possible to predict the difference of re-embrittlement in comparison with primary embrittlement simply by suppressing the Cu term during re-embrittlement after annealing. The behaviour obtained reproduces qualitatively well the behaviour shown by high P welds of VVER-440, see Fig. 11.

6. Conclusion

An analytical model based on the three key mechanisms involved in radiation embrittlement has been tested on a large set of data on both Ni-free and Ni-containing model alloys, irradiated at two different fluences in the HFR Petten and in Kola NPP.

The model parameters for the precipitation and segregation terms in Ni-free alloys are linearly related with the Cu and P contents, respectively.

In order to reproduce the higher shifts of DBTT and their rate of increase with the accumulated fluence observed in Ni alloys, it is assumed that Ni amplifies the parameters controlling embrittlement by damage in the matrix and by precipitation. On the one hand a linear dependence on Ni for the matrix damage term is found, on the other hand the synergism of Ni with Cu is made possible by including a dependence on Ni in the form of $Ni^{0.35}$ for contents above 1 wt% in the precipitation parameter.

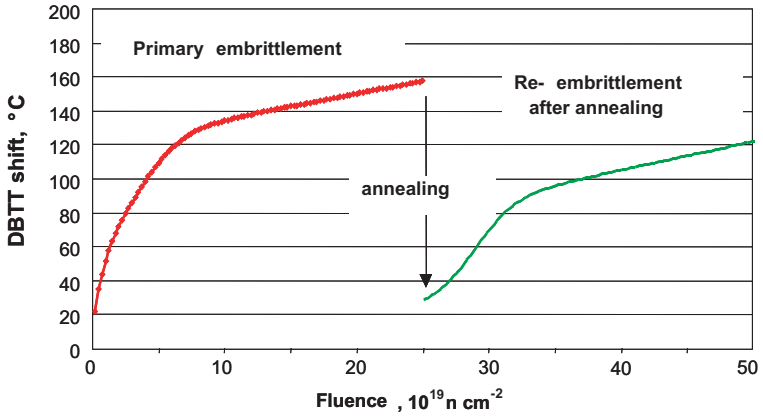

Fig. 11. Schematic of primary radiation embrittlement and re-embrittlement calculated with proposed model.

References

[1] G.R. Odette, Scr. Met. 17 (1983) 1183.
[2] M.K. Miller, M.G. Burke, Warrendal, PA: TMS-AIME, 1988, p. 141.
[3] C.A. English, S.R. Ortner, G. Gage, W.L. Server, S.T. Rosinski, in: ASTM STP 1405, West Conshohocken, PA, 2001, p. 151.
[4] J. Ahlf, A. Zurita, High Flux Reactor (HFR) Petten – Characteristics of the installation and the irradiation facilities, Report EUR 15151, 1993.
[5] L. Debarberis, K. Törrönen, F. Sevini, B. Acosta, A. Kryukov, Y. Nikolaev, M. Valo, in: Proc. 6th International Conference on Materials Issues in Design, Manufacturing and Operation of NPP Equipment, St. Petersburg, Russia, CRISM 'Prometey', 19–23 June 2000.
[6] L. Debarberis, F. Sevini, B. Acosta, A. Kryukov, Y. Nikolaev, A.D. Amaev, M. Valo, Int. J. Pressure Vessels Piping 79 (2002) 637.
[7] L. Debarberis, A. Kryukov, D. Erak, Y. Kevorkyan, D. Zhurko, Int. J. Pressure Vessels and Piping 81 (2004) 695.
[8] L. Debarberis, A. Kryukov, F. Gillemot, M. Valo, A. Morozov, M. Brumovsky, B. Acosta, F. Sevini, Int. J. Strength Mater. 3 (2004) 65.
[9] A. Kryukov, D. Erak, Y. Shtrombakh, L. Debarberis, M. Valo, J. Kohopaa, S. Vodenicharov, in: Proc. NATO Advanced Research Workshop, Kiev, Ukraine, National Academy of Sciences of Ukraine, Institute for Problems of Strength, 2002.
[10] J.R. Hawthorne, Report of Joint Coordinated Committee on Civilian Nuclear Reactor Safety, Rockville, Maryland, USA, 1991.